Bull. Chem. Soc. Jpn., 71, 1483—1499 (1998)

Accounts

Chemical Processes in Solution Studied by an Integral Equation Theory of Molecular Liquids

Fumio Hirata

Department of Theoretical Study, Institute for Molecular Science, Okazaki, 444-8585

(Received March 4, 1998)

A variety of chemical processes in solution is explored theoretically by means of the extended RISM equation, an integral equation theory of molecular liquids. The chemical processes include the classical problem of ion hydration, solvent induced electronic structure change and chemical reactivity in solution, protein folding, and dynamics of solvent as well as solvated ions. A special emphasis is laid on the ability of the theory to account for chemical specificities of molecules, which is crucial for any chemical processes in solution.

The infinitely large variety of molecular species produced from a rather limited number of chemical elements through chemical reactions is a fact that has fascinated chemists and motivated most of their research. The electronic structure and its changes are of course the primary cause of such a variety in chemical compounds. There is, however, another important factor, collectively refered to as the "solvent effect," which plays a crucial role in determining the direction and rate of chemical reactions in solutions. It is not surprising that so much effort has been put on evaluating "solvent effect" in many fields including organic and biological chemistries, if one considers that most chemical reactions take place in the environment of solutions.[1,2]

The phenomenological models or the dielectric continuum models represented by the Born model for ion hydration,[3] Onsager's reaction field,[4] and the Stokes–Einstein–Debye law[5—7] for non-equilibrium processes have long been standard tools in evaluating such solvent effects. The Marcus theory for the electron transfer reaction may be the best example of such models.[8] The dielectric continuum models aided with highly sophisticated computational algorithms are exploited even for the most challenging problems in chemistry such as chemical reactions and protein stability.[2,9,10] However, the latest developments in the experimental techniques and the molecular simulations have unequivocally revealed the serious breakdown of such models: The interpretation of such experimental data is reaching a point where the continuum description fails to reconcile the disagreement between experiment and the models without making use of unphysical parameters.[11—13]

The statistical mechanics of liquids and liquid mixtures is the most natural choice for replacing the phenomenological models. The liquid state theories should be able to handle the specificity of molecules in order for the theories to make sense to chemists. However, until about thirty years ago, the theory of liquid is largely limited to a system of spherical molecules, the best example of which is a system of hard spheres.[14] The chemical characteristics of a system are represented just by the diameter of a molecule, which of course does not satisfy the demands from chemistry. This is one of the reasons why the statistical mechanics could not have replaced the continuum models; theories based on the phenomenological models are still predominantly used in the field of chemistry to interpret experiments. The major breakthrough toward the liquid state theory in chemistry has been made by D. Chandler and H.C. Andersen in 1971 with their theory for the reference interaction site model (RISM).[15] The theory is a natural extension of the Ornstein–Zernike (OZ) equation to a mixture of atoms, but with strong intramolecular correlations which represent chemical bonds. The theory takes account of one of the two important chemical aspects of molecules, geometry, in terms of the intramolecular correlation. However, it does not handle the other chemical aspect of molecules, electrostatics, in its original forms. The charge distribution in a molecule, which is a classical manifestation of the electronic structure, plays a dominant role in determining the chemical specificity of the molecule. Therefore, without including the charge distribution in molecules, the description is incomplete in terms of chemical specificity. A complete chemical characterization of molecular liquids became possible in 1981 due to the appearence of the extended RISM theory which takes the charge distribution as well as the molecular geometry into account.[16] The electrostatic interactions between atoms, a naive treatment of which causes

divergence in the spatial integrals in the OZ type equations, has been handled by a renormalization technique originated by J. Mayer,[17] implemented in the Ornstein–Zernike equations by Allnat,[18] and fully explored by H.L. Friedman and his coworkers[19] in their theories of the electrolyte solution. In that sense, the extended RISM theory is also an natural extension of the Mayer–Allnat–Friedman electrolyte solution theory to the molecular liquids. Applications of the theory to a variety of liquids and solutions have demonstrated its capability of describing the chemical specificity of liquids in a molecular detail. Such application includes analyses of water structure,[20] solvation free energy of ions,[21,22] the B–Z transition of DNA,[23] S_N2 reactions,[24] the dynamic structure factor of water,[25] the dynamic Stokes shift,[26] and the stability of polypeptides.[27,28]

In this article, I present our recent efforts to explore a variety of chemical processes in solution by means of the extended RISM theory. In the following section, the extended RISM theory is briefly summarized for the purpose of providing definitions of the physical variables used throughout the paper. In Section 2, the classical problem of ion hydration is revisited from a microscopic point of view. A special stress is laid on how the classical concepts of ion hydrations, such as the "negative hydration" and the "structure breaking" effect, are accounted for by the modern statistical mechanics of liquids. Section 3 is devoted to the solvent induced change in electronic structure of molecules in solution as well as solvent effects on chemical reactions. The stability of biomolecules in solution is discussed in Section 4, where roles of solvent in determining protein conformations are investigated by means of a combined RISM and Monte Carlo method. In Section 5, non-equilibrium aspects of solutions are studied based on the RISM theory coupled with the generalized Langevin equation. The dynamics of a solvated ion in polar liquids is investigated from the viewpoint of collective density fluctuations in solvents.

1. Density Fluctuations in Molecular Liquids

When liquids are viewed as a collection of molecules (or atoms) rather than a continuum, the molecular (atomic) density fluctuates in space as well as in time. The local density or the density field is defined as

$$\rho_\alpha(\boldsymbol{r}) = \sum_j \delta(\boldsymbol{r} - \boldsymbol{r}_j^\alpha), \tag{1}$$

where $\rho_\alpha(\boldsymbol{r})$ denotes the density of atom type α at the position $\boldsymbol{r}$, δ indicates the Dirac δ-function, and the sum runs over all molecules in the system. In uniform liquids, the thermal average of the density field is constant, namely,

$$\langle \rho_\alpha(\boldsymbol{r}) \rangle = \rho_\alpha, \tag{2}$$

and this quantity does not carry microscopic information concerning liquid structure. It is the variance and covariance of the density fluctuation, defined by $\chi_{\alpha\beta}(\boldsymbol{r},\boldsymbol{r}') = \langle \delta\rho_\alpha(\boldsymbol{r})\delta\rho_\beta(\boldsymbol{r}') \rangle$, that characterizes the microscopic structure of liquids, where $\delta\rho_\alpha(\boldsymbol{r})$ is defined as,

$$\delta\rho_\alpha(\boldsymbol{r}) = \rho_\alpha(\boldsymbol{r}) - \langle \rho_\alpha(\boldsymbol{r}) \rangle. \tag{3}$$

$\chi_{\alpha\beta}(\boldsymbol{r},\boldsymbol{r}')$ can be split into intra- and inter-molecular contributions as

$$\chi_{\alpha\beta}(\boldsymbol{r},\boldsymbol{r}') = \omega_{\alpha\beta}(\boldsymbol{r},\boldsymbol{r}') + \rho h_{\alpha\beta}(\boldsymbol{r},\boldsymbol{r}'), \tag{4}$$

where $\omega_{\alpha\beta}(\boldsymbol{r},\boldsymbol{r}')$ and $h_{\alpha\beta}(\boldsymbol{r},\boldsymbol{r}')$ represent the intra and intermolecular correlation functions, respectively.

For the uniform liquids in which the translational and rotational invariance are implied, the $\omega_{\alpha\beta}(\boldsymbol{r},\boldsymbol{r}')$ and $h_{\alpha\beta}(\boldsymbol{r},\boldsymbol{r}')$ can be just functions of the distance between the two positions, $\boldsymbol{r}$ and $\boldsymbol{r}'$, namely,

$$h_{\alpha\beta}(\boldsymbol{r},\boldsymbol{r}') = h_{\alpha\beta}(|\boldsymbol{r} - \boldsymbol{r}'|), \tag{5}$$

and

$$\omega_{\alpha\beta}(\boldsymbol{r},\boldsymbol{r}') = \omega_{\alpha\beta}(|\boldsymbol{r} - \boldsymbol{r}'|). \tag{6}$$

The RISM theory provides a method to calculate the intermolecular correlation function $h_{\alpha\beta}(r)$ given the interaction potential between a pair of molecules, which is represented by a sum of the site–site interactions,

$$u(1,2) = \sum_\alpha \sum_\beta u_{\alpha\beta}(r), \tag{7}$$

and the molecular geometry which is represented by $\omega_{\alpha\beta}(r)$.[15] In the case of rigid molecules, ω can be expressed by

$$\omega_{\alpha\beta}(r) = \rho_\alpha \delta_{\alpha\beta}\delta(r) + (1 - \delta_{\alpha\beta})\frac{1}{4\pi L_{\alpha\beta}^2}\delta(r - L_{\alpha\beta}), \tag{8}$$

where $L_{\alpha\beta}$ denotes the rigid constraints, or "bond length" between an atom pair α and β.

A general expression of the RISM equation for a system consisting of several molecular species can be written as,[16]

$$\boldsymbol{\rho h \rho} = \boldsymbol{\omega} * \boldsymbol{c} * \boldsymbol{\omega} + \boldsymbol{\omega} * \boldsymbol{c} * \boldsymbol{\rho h \rho}, \tag{9}$$

where $\boldsymbol{\rho}$ denotes a diagonal matrix consisting of the density of molecular species, $\boldsymbol{c}$ and $\boldsymbol{h}$ are the direct and total correlation matrices, respectively, of which each element, say, $h_{\alpha\beta}$ stands for the correlation function between an intermolecular atom pair α and β. The asterisk indicates the convolution integrals and matrix products. For a problem of solvent effect on chemical processes in solution, the most interesting case is the infinite dilution limit in which the concentration of the chemical species of interest tends to zero. In such a case, the general expression becomes

$$\boldsymbol{h}^{vv} = \boldsymbol{w}^v * \boldsymbol{c}^{vv} * \boldsymbol{w}^v + \boldsymbol{w}^v * \boldsymbol{c}^{vv} * \boldsymbol{\rho}^v \boldsymbol{h}^{vv}, \tag{10}$$

$$\boldsymbol{h}^{uv} = \boldsymbol{w}^u * \boldsymbol{c}^{uv} * \boldsymbol{w}^v + \boldsymbol{w}^u * \boldsymbol{c}^{uv} * \boldsymbol{\rho}^v \boldsymbol{h}^{vv}, \tag{11}$$

where subscripts "u" and "v" indicate sol"u"te and sol"v"ent, and $\boldsymbol{w} = \boldsymbol{\omega}\boldsymbol{\rho}^{-1}$. Those equations are supplemented by closure relations such as the Percus–Yevick (PY) and the hypernetted chain (HNC) approximations, namely,

$$c_{\alpha\beta}(r) = \exp[-\beta u_{\alpha\beta}(r)]\{1 + h_{\alpha\beta}(r) - c_{\alpha\beta}(r)\} - \{h_{\alpha\beta}(r) - c_{\alpha\beta}(r)\} - 1 \quad \text{(PY)} \tag{12}$$

and

$$c_{\alpha\beta}(r) = \exp[-\beta u_{\alpha\beta}(r) + h_{\alpha\beta}(r) - c_{\alpha\beta}(r)] - \{h_{\alpha\beta}(r) - c_{\alpha\beta}(r)\} - 1 \quad \text{(HNC)} \tag{13}$$

For the applications of the theory to the polar liquids in which the Coulombic interactions are essential, the equations are renormalized (extended RISM) to avoid divergence regarding the spatial integral.[16]

All thermodynamic functions can be calculated from the pair correlation functions. The excess chemical potential or the solvation free energy of a molecule has particular importance in determining the stability of the molecule in solution.[29]

$$\Delta\mu = -\frac{\rho}{\beta}\sum_{\alpha s}\int d\boldsymbol{r}[c_{\alpha s}(r) - \frac{1}{2}h_{\alpha s}(r)^2 + \frac{1}{2}h_{\alpha s}(r)c_{\alpha s}(r)] \tag{14}$$

The Lennard–Jones (L–J) plus Coulomb interaction,

$$u_{\alpha\beta}(r) = 4\epsilon_{\alpha\beta}\left[\left(\frac{\sigma_{\alpha\beta}}{r}\right)^{12} - \left(\frac{\sigma_{\alpha\beta}}{r}\right)^{6}\right] + \frac{q_\alpha q_\beta}{r}, \tag{15}$$

are employed for the site-site pair interaction throughout the text, where $\epsilon_{\alpha\beta}$, $\sigma_{\alpha\beta}$, q_α, and q_β have usual meanings. The standard OPLS-type[30] parameters are used in most of the calculations except for the section five, where we adopt ECEPP-type[31] parameters for the interaction potential of peptide due to a historical reason associated with our research collaboration. For water potential, three different sets of parameters, TI3P,[32] SPC,[33] and SPC/E,[34] are employed in the different problems discussed below. I believe, however, those differences in the potential parameters do not affect the conclusions drawn in the paper; the conclusions are all qualitative and small changes in the numbers do not make any difference. In all cases, the standard combination rules, $\epsilon_{\alpha\beta} = (\epsilon_\alpha\epsilon_\beta)^{1/2}$ and $\sigma_{\alpha\beta} = (\sigma_\alpha + \sigma_\alpha)/2$, are employed to estimate the L–J parameters for a pair of different atoms.

2. Solvation of Ions and Hydrophobic Solutes

Most fundamental physicochemical processes in solution would be solvation of ions. Especially, hydration of ions has been a major concern since Drude–Nernst (1894) and Born[3] due to its close relation with chemical reactions.[8] Two closely related models for a microscopic picture of the hydration have been proposed in the 1957 issue of the Discussion Faraday Society.[35,36] Frank and Wen[35] proposed a model based on the solvation thermodynamics, according to which a small ion like Li^+ is surrounded by three concentric regions. The innermost (region A) is the region where water molecules are firmly bound to the ion, the second (region B) is the region in which water is less "ice-like," i.e. more random in organization, than "normal water", and the third (region C) contains normal water polarized in the ordinary way by the ionic field which becomes relatively weak. They presumed that the cause of the structure-breaking effect is an approximate balance in the region B between two competing orientational effects which act on water molecules: the hydrogen-bonding with neighboring water molecules, and the orienting influence upon the dipole of the spherically-symmetrical ionic field. All three regions appear around a small ion such as the Li^+ ion, while only B and C regions can be seen in case of larger ions such as Cl^- ion, since the A-region is hidden by the atomic core. In the same issue, Samoilov[36] proposed a similar picture for the ion hydration but from a different point of view. Samoilov could abstract activation energies (E_i) associated with the activated jump of water molecules from the immediate vicinity of an ion to the bulk from experimental data of the diffusion constant and the viscosity. Comparing E_i with the same quantity but with a water molecule in place of an ion, which is denoted by E_0, Samoilov found that $E_i > E_0$ for small ions such as Li^+ and Na^+ while $E_i < E_0$ for large ions like K^+ and Cl^- ions. Samoilov referred to the two cases, ΔE_i $(= E_i - E_0) > 0$ and $\Delta E_i < 0$ as "positive" and "negative" hydration, respectively. Those two pictures regarding the ion hydration proposed four decades ago have given great influence on interpreting experiments in the field of solution chemistry and still do.[37] However, it is still ambiguous what those concepts like "negative hydration" and "structure breaking" realy mean in terms of the microscopic picture of solvent around the ions. It is of interest to see how the phenomena can be characterized in terms of the integral equation method.[38]

The logarithm of the radial distribution function (RDF), $g(r)$ $(= h(r) - 1)$, multiplied by $-k_B T$ is the potential of mean force or the solvent averaged potential surface. The transition from the first to the second minimum of the potential of mean force can be regarded as the activation jump of the sort modeled by Samoilov, and the energy difference between the first minimum and the first maximum is then an activation energy. The potential of mean forces between ion and water and those between water molecules, which can be calculated from the extended RISM equation, give the activation energy associated with the jump, which has been empirically obtained by Samoilov. Figure 1 shows the difference in activation energy ΔE_i which are obtained from the ion-oxygen distribution function for cations and the ion-hydrogen distribution function for anions. It can be readily seen that the picture for the ion hydration proposed by Samoilov is qualitatively reproduced by the theory (Table 1). The relative residence time calculated from a simple formula of the

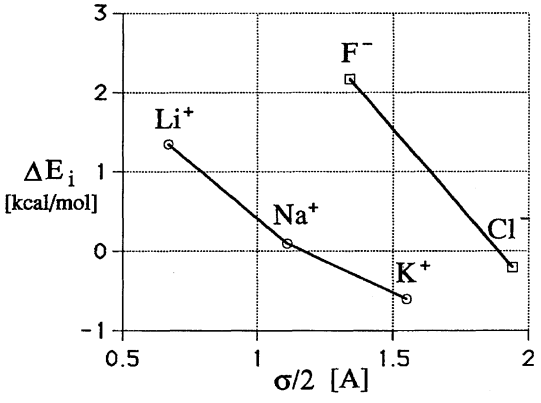

Fig. 1. ΔE_i's for various ions.

Table 1. Activation Energy (ΔE_i) for Various Ions. (Unit in kcal mol^{-1})

Ion	$\Delta E^{a)}$ (ex-RISM)	$\Delta E^{b)}$ (experiment)
Li^+	1.35	0.73
Na^+	0.10	0.25
K^+	−0.60	−0.25
F^-	2.17	
Cl^-	−0.20	−0.27

a) The results obtained from ex-RISM (Ref. 38). b) Experimental results by Samoilov (Ref. 36).

transition state theory:

$$\frac{\tau_i}{\tau_0} = \exp(\Delta E_i / k_B T), \tag{16}$$

shows reasonable agreement with those obtained by Samoilov. All those observations indicate that the old concepts for ion hydration have some basis which can be interpreted theoretically in terms of the potential of mean force. Then, the next question to be asked is "Is it possible to characterize the structural modification of solvent around the ions?"

In Fig. 2, plotted are the solvent-solvent radial distribution functions (RDF) for water between O–O atoms and between O–H atoms, and the perturbation on RDFs due to existence of ions calculated from the extended RISM equation. The perturbations due to ions or the density derivatives of the RDF are calculated using the Yu–Karplus method.[39] Only the results for Li^+ and Cl^- are shown; these represent, respectively, the ions of positive and negative hydrations. The structural characteristics of water are manifested in two features in the RDFs: The sharp peak around 1.4 Å in the O–H RDF and the small dent around 4.2 Å in the O–O RDF.

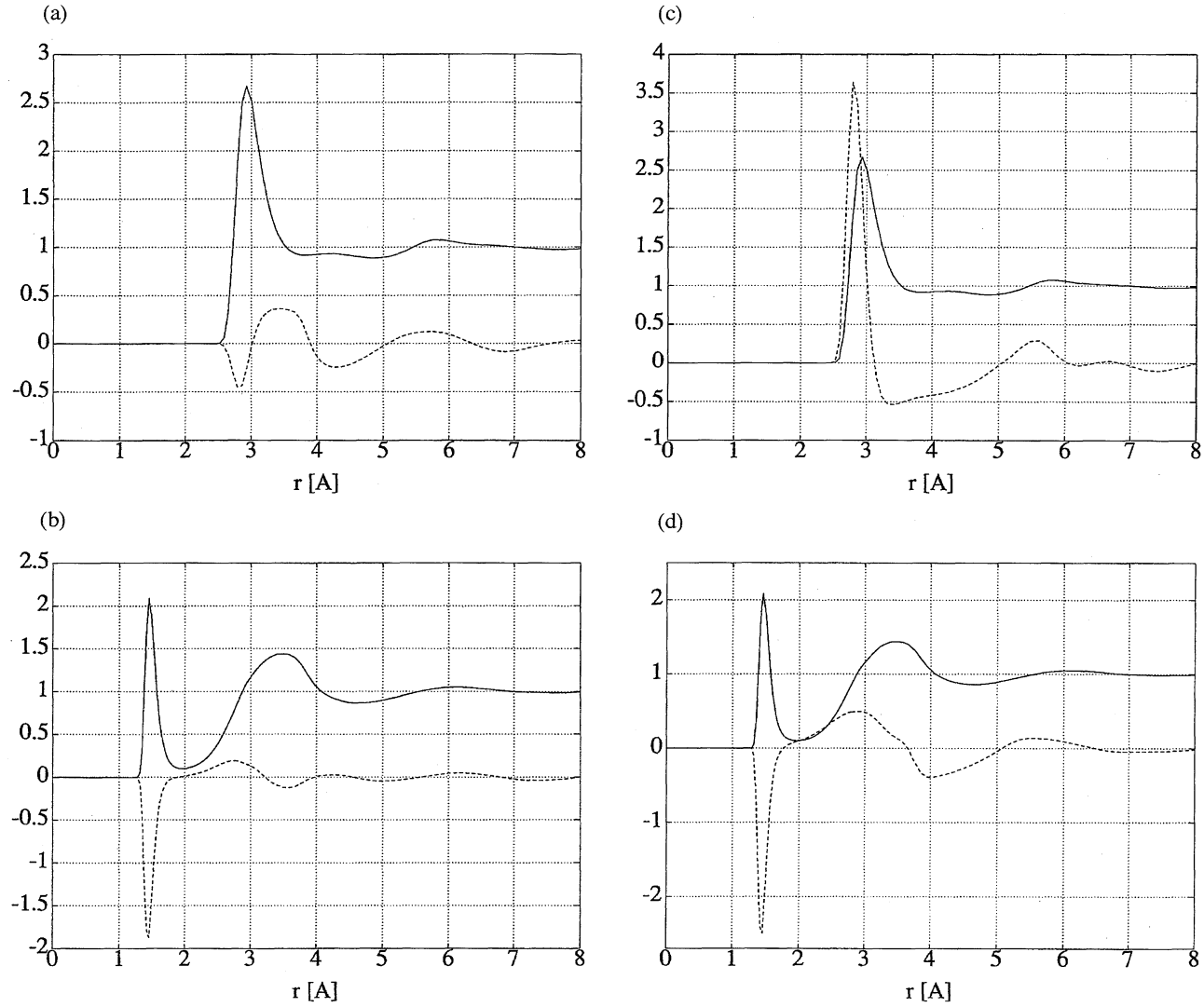

Fig. 2. (a and b) Solvent radial distribution functions and their derivatives with respect to the density of Li^+; (a) g_{OO} (solid line) and its density derivative (dashed line); (b) g_{OH} (solid line) and its density derivative (dashed line). (c and d) Solvent radial distribution functions and their derivatives with respect to the density of Cl^-; (c) g_{OO} (solid line) and its density derivative (dashed line); (d) g_{OH} (solid line) and its density derivative (dashed line).

The first feature is due to the hydrogen-bond between a pair of molecules, and the second one is a manifestation of the three-body correlation in the hydrogen-bond network in water, which has an ice-like tetrahedral coordination. It was undoubtedly a major triumph for the extended RISM theory to reproduce such features of water structure without using *ad hoc* models; such a feat had long been considered as a main goal for the liquid state theory.[16,20] The ion perturbation depicted by the dotted lines characterizes the way how those features of water structure are modified. As can be clearly seen, the peak around 1.4 Å in the O–H RDF is disrupted in either case due to the ion perturbation. It is not surprising because in both cases the solvent–solvent hydrogen-bond is weakened due to the orientational effect of the ionic field. Then, what distinguishes the negative from positive hydrations? This question can be answered by examining the O–O RDF. The comparative inspection of the density derivative curves for Li^+ and Cl^- indicates that the first peak of the O–O RDF shifts outward for Li^+ while it displaces inward for Cl^-. What physical significance can be attached to this observation? When an ion is positively hydrated as in case of Li^+, water molecules around the ion tend to align the dipole moments in parallel to the ion field. The water molecules will then repell each other due to the repulsive electrostatic interactions between O–O and between H–H, which will appear as the outward shift of the O–O RDF. On the other hand, when the negative hydration occurs as in case of Cl^-, the equilibrium of water structure shifts toward that with less "tetrahedral" coordination, which is denser than the ice-like structure. The phenomenon is analogous to the heat perturbation which causes the maximum density at 4 °C. The combination of the shift in the first peak of the O–O correlation and the sign of the change in the first peak of the O–H correlation as well as the second peak of the O–O correlation characterizes the modification of the solvent structure around ions.

It is interesting to see from such a viewpoint how the water–water correlation function is modified around a hydrophobic solute. In Fig. 3, we plotted such correlation functions for methane as the solute. The first peak of the O–H correlation increases around the hydrophobic solute indicating that the hydrogen-bond is strengthened. On the other hand, the first peak of the O–O correlation function shifts inward, indicating that the water density is increased around the solute. This observation implies that the water structure is in fact increased around the nonpolar solute, as has been widely accepted. However, the modified structure is not ice-like but some structure which has higher density than that characteristic of the tetrahedral coordination. Those changes in the pair correlation function due to the ion perturbations are summarized in Table 2. It can be readily seen that the classical models of ion hydration are well characterized in terms of the ion perturbation to the pair correlation function of water.

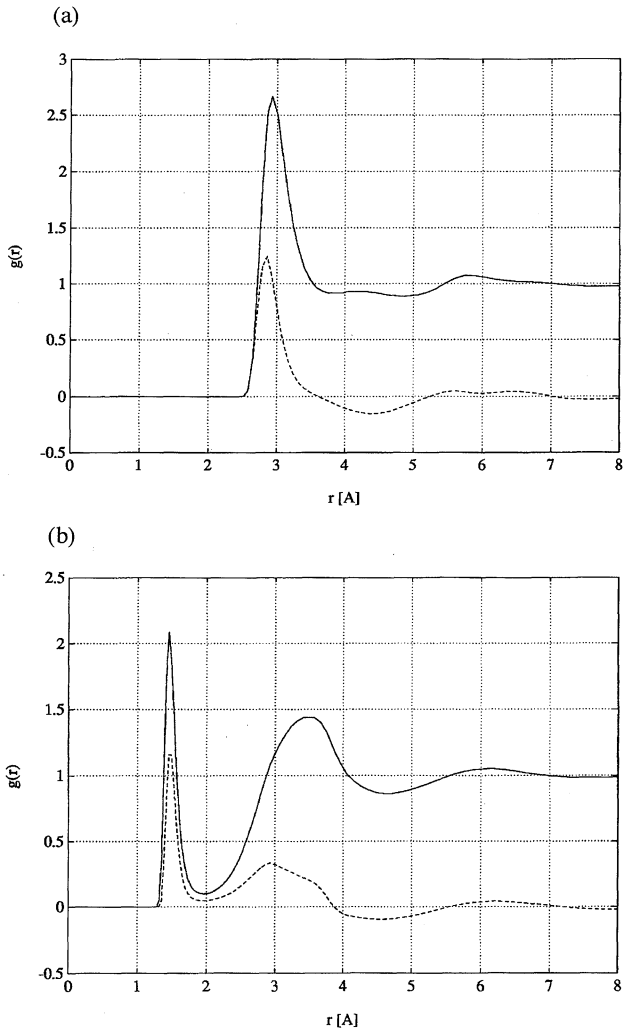

Fig. 3. Solvent radial distribution functions and their derivatives with respect to the density of methane; (a) g_{OO} (solid line) and its density derivative (dashed line); (b) g_{OH} (solid line) and its density derivative (dashed line).

Table 2. Characteristics of Ion Perturbation to Water Structure

	Positive hydration	Negative hydration	Hydrophobic hydration
O–O First peak	→	←	+
O–O Second peak	–	–	–
O–H First peak	–	–	+

a) → outward shift, b) ← inward shift, c) + peak increases, d) – peak decreases.

3. Electronic Structure of Solvated Molecules and Chemical Equilibrium

Chemical reactions are undoubtedly the most important issue in theoretical chemistry, in them the electronic structure plays an essential role. As long as molecules in the gas phase are dealt with, the theory for the electronic structure has been enjoying great success. However, when it comes to molecules in solution, the stage of theory is still that of an infant. Since it is impossible to solve the Schrödinger equation

for an entire system including about 10^{23} solvent molecules, the most promising approach so far is some type of hybrid between the classical solvent and quantum solute. Roughly three types of hybrid approaches have appeared depending on how to treat the solvent degrees of freedom: molecular simulations, continuum models, and the integral equations. The continuum models employ the electrostatic theory in order to evaluate the reaction field exerted on the solute from the continuum dielectrics regarded as a solvent.[9] A variety of different methodologies including Onsager's reaction field, Born's model[40] and the image charge models[41] have been implemented for the reaction field. An obvious advantage of the method is its handiness, and a disadvantage is an artifact introduced at the boundary between solute and solvent. The molecular simulation techniques do not suffered from such an artifact. However, they have their own disadvantages, the obvious one being computational load added to the already heavy calculation of the electronic structure. The integral equation method is free from such disadvantages, and gives a microscopic picture for the solvent effect on the electronic structure of a molecule within a reasonable amount of computation time.[42,43]

Defining the energy of a molecule by the sum of the electronic energy, $\langle \Psi|H|\Psi\rangle$, and nuclear repulsion energy, E_{nuc},

$$E_{\mathrm{solute}} = \langle \Psi|H|\Psi\rangle + E_{\mathrm{nuc}}, \tag{17}$$

where the total wave function $|\Psi\rangle$ is represented by a Slater determinant of molecular orbitals, $\{\psi_i\}$, we can derive the Fock operator for an isolated molecule in gas phase from the variational principle,

$$\delta(E_{\mathrm{solute}} - [\text{orthonomality constraints for } \{\psi_i\}]) = 0. \tag{18}$$

Similarly, the Fock operator for a solute molecule in solvent can be derived in the same manner as in gas phase from a variational principle,[43]

$$\delta(A - [\text{orthonomality constraints for } \{\psi_i\}]) = 0, \tag{19}$$

where A is the Helmholtz free energy defined by

$$A = E_{\mathrm{solute}} + \Delta\mu. \tag{20}$$

In Eq. 20, E_{solute} and $\Delta\mu$ are the energy of solute under solvent influence defined by Eq. 17 and the solvation free energy defined by Eq. 14, respectively. The Fock operator with solvent effect derives naturally from the variational procedure to read:

$$F^{\mathrm{s}} = F^{\mathrm{g}} - \sum_{\lambda\in u} V_\lambda b_\lambda, \tag{21}$$

where the first term is the Fock operator for an isolated molecule, and the second term represents the solvent effect. In the second term, b_λ is a population operator of solute atoms and the V_λ represents the potential of the electrostatic reaction field at solute atom λ produced by solvent molecules. The potential of the reaction field takes a microscopic expression in terms of the site-site radial distribution functions between solute and solvent.

$$V_{\lambda\in u} = \rho\sum_{\alpha\in v}\int_0^\infty \frac{q_\alpha}{r} g_{\lambda\alpha}(r) 4\pi r^2 \mathrm{d}r, \tag{22}$$

where α and λ specify solvent and solute sites, respectively, and ρ denotes the solvent density. The site-site radial distribution functions $g_{\lambda\alpha}(r)$ can be calculated from the extended RISM equations, Eqs. 10 to 12.

The statistical solvent distribution ($g_{\lambda\alpha}$) around the solute is determined by the electronic structure (Ψ) or the partial charges of the solute, while the electronic structure of the solute is influenced by the solvent distribution. Therefore, the Hartree–Fock equation and the RISM equation should be solved in a self-consistent manner. It is this self-consistent determination of the solute electronic structure and the solvent distribution that the RISM-SCF procedure features.

One of the concerns which are common to this type of hybrid approaches is an error associated with determination of charge distribution. Since electrons have only the probability distribution at certain position in a molecule and the RISM calculation requires the delta-function-like distribution at a site, it is necessary to translate the continuous probability distribution to partial charges at discrete positions. The Mulliken population analysis which have been widely employed in earlier work is notorious for giving a wrong estimate of electrostatic field around the molecule. The partial charges in the RISM-SCF procedure are determined in such way that the electrostatic potential produced by the partial charges at grid points around the solute molecule best agree with that calculated from the wave functions in a sense of the least square fitting (LSF). It has been observed from the few applications performed so far that the LSF procedure gives a reasonably good estimate for charge distribution. An example of estimated charge distribution is shown in Table 3 in terms of dipole moments. The method has been successfully applied to several problems in which solvent effects on the electronic structure play a significant role; such applications include the solvato-chromism of formaldehyde,[42] the coupled substitution and solvent effects on basicity and

Table 3. Dipole Moments of Methylamines and Protonated Methylamines (in Debye Unit)[a]

	In gas phase			In aqueous solution	
Species	DMI[b]	DPC[c]	Exp.[d]	DMI	DPC
NH_3	1.82	1.86	1.47	2.57	2.60
$(CH_3)NH_2$	1.47	1.37	1.24 or 1.35	2.02	1.92
$(CH_3)_2NH$	1.11	1.22	1.03	1.96	2.08
$(CH_3)_3N$	0.74	0.88	0.67	1.60	1.78
NH_4^+	0.00	0.00		0.00	0.01
$(CH_3)NH_3^+$	2.23	2.18		2.65	2.59
$(CH_3)_2NH_2^+$	1.50	1.48		1.95	1.92
$(CH_3)_3NH^+$	0.87	0.90		1.27	1.30

a) Dipole moments of protonated methylamines are calculated with respect to center of Mass. b) Dipole moment calculated from the wave function through molecular integral. c) Dipole moment calculated from the partial charges. d) Experimental data in gas phase. (R.C. Weast et al.," CRC Handbook of Chemistry and Physics," CRC Press, Inc. Florida (1989)).

acidity,[44,45] the ab initio determination of electronic and liquid structure of water,[46] and temperature dependence of the auto-ionization coefficient of water.[47] Among those applications, I briefly review a study on the classical problem of the substitution effect on the basicity of the methylamines.[44]

It is experimentally well known that the basicity of the methylamines increases monotonically with successive methyl substitutions in the gas phase, and that the order reverses at the trimethylamine in aqueous environment.[48] The monotonic increase of the basicity in the gas phase has been explained in terms of the "negative induction" or the polarization effect[49] due to the methyl groups.[50,51] There are essentially two important factors to be considered as the solvent effect on the proton affinity; the solvation free energy and the energy change associated with the electron reorganization upon solvation. The solvation free energy in turn consists of the solute–solvent interaction energy and the free energy change associated with the solvent reorganization. Employing the thermodynamic cycle depicted in Fig. 4, the free energy changes associated with the protonation of the methylamines relative to those of ammonia are calculated and plotted in Fig. 5 against the increasing number of the methyl groups. The contribution $\Delta\Delta G^{s}_{298}$ (solute) from solute itself exhibits similar monotonic behavior with the gas

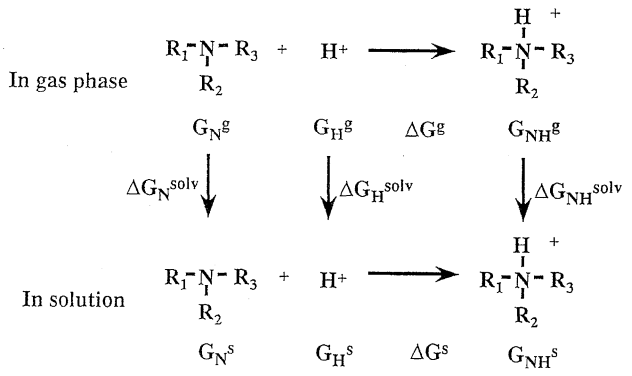

Fig. 4. The thermodynamic cycle with respect to the protonation of methylamines in gas phase and in aqueous solution.

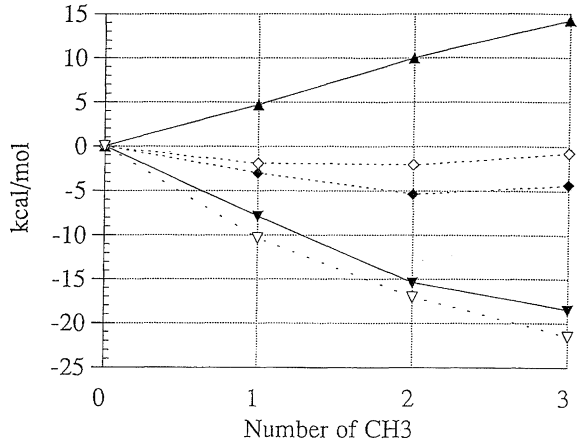

Fig. 5. Free energy changes upon protonation referred to NH_3: ▽, $\Delta\Delta G^{g}_{298}$; ▼, $\Delta\Delta G^{s}_{298}$ (solute); ▲, $\Delta\Delta G^{s}_{298}$ (solvent); ◆, $\Delta\Delta G^{s}_{298}$; ◇, experimental data.

phase result $\Delta\Delta G^{g}_{298}$ which is in good agreement with the experiments. The difference between $\Delta\Delta G^{s}_{298}$ (solute) and $\Delta\Delta G^{g}_{298}$ is due essentially to the electron reorganization energy. The solvation free energy $\Delta\Delta G^{s}_{298}$ (solvent) shows the monotonic increase with the successive methyl substitution. The sum of the two contributions produces the inversion in the overall free energy change $\Delta\Delta G^{s}_{298}$, which is in qualitative accord with the experimental result.

4. Solvation of Biomolecules

One of the most promising applications to which the extended RISM theory can make potentially important contributions is the solvation of biomolecules. For biomolecules such as protein, it is a final goal for biochemistry to explore the relation between their conformations and biological functions. The first important step toward the goal would be to explain the conformational stability of biomolecules in terms of the microscopic structure of the molecules in solvent. It is an extremely difficult problem by any means due to the overwhelmingly large degrees of freedom to be handled, including protein and solvent. As for the small and/or short-time fluctuations of protein around the native structure, a variety of molecular simulation techniques provide quite powerful tools to explore the microscopic structure of protein and solvent.[52] However, the techniques may not be applied straightforwardly to a process in which large conformational fluctuation of biomolecules is concerned. The most well-regarded process in such cases is the so called "protein folding"; namely, a protein in a denatured state folds into its native conformation by changing the thermodynamic conditions such as temperature and ionic strength of the solution.[53] The process was first demonstrated unambiguously by Anfinsen; it suggests strongly that the primary structure or the amino-acid sequence contains sufficient information for a protein to fold into its unique native conformation.[54]

There are two well documented difficulties in the protein folding. One of those concerns the multi-minima nature of the energy surface of proteins, which prevents a molecular simulation from sampling large conformation space of the molecule due to "trapping" in a local minimum.[55] The problem has been solved essentially by recent developments in a variety of sampling methods based on generalized ensembles in the Monte-Carlo simulation.[55–58] However, the final goal of protein folding may not be achieved unless the other important problem is solved, which is concerned with the solvent.[59] A protein may fold into "some" conformation with an overlysimplified solvent model, or even without any solvent. However, if the "protein folding" is defined as a process to make a "unique" native conformation, such methods with over-simplified solvent models will never attain the successful goal. What determines the unique conformation of native protein is the chemical specificity of each of twenty amino-acids. But, this is not the whole story. The solvent, water, is as specific in chemical nature as amino acids.[59] Therefore, it should be considered that the unique conformation of native protein is made by a cooperative interaction of those specificities in protein and solvent. From such considerations,

the solvent model for protein folding should satisfy two requirements. Firstly, the calculation of solvation free energy should be reasonably fast so that a computer can sample a wide range of the free energy surface to find the native conformation. Secondly, the solvent–solvent and solute–solvent interactions should properly account for chemical specificities of peptides and water such as hydrogen-bonds so that the uniqueness of native conformation is not sacrificed. Molecular simulations with explicit solvent molecules fail to satisfy the first requirement.[52] Methods with over-simplified solvent models such as so called minimum model and the continuum dielectric model do not meet the second requirement.[10,60] Successful methods which satisfy both requirements should be those in which the solvent degrees of freedom are coarse-grained by means of the statistical mechanics with proper account of the chemical specificity of solvent molecules. The RISM theory can undoubtedly be one of such methods which meet both requirements.

We have recently started to explore the possibility of applying the RISM theory to the protein folding.[61,62] The method consists of two theoretical ingredients. One is the Monte-Carlo algorithms based on the generalized ensembles, which enable us to sample a wide range of conformational space of protein without being trapped in local minima.[57,58] The other is the RISM theory to calculate the solvation free energy. The free energy surface $F(\{M\})$ of protein can be expressed by

$$F(\{M\}) = E_{\mathrm{conf}}(\{M\}) + \Delta\mu(\{M\}), \tag{23}$$

where $\{M\}$ represents a conformation of protein, and $E_{\mathrm{conf}}(\{M\})$ and $\Delta\mu(\{M\})$ respectively denotes the potential energy of protein in vacuum and the solvation free energy.

As a preliminary step toward the protein folding, we have carried out the Monte-Carlo simulation for Met-enkephaline in various environments including vacuum, water, and non-polar solvent. A key to the success of the simulation was to develop a rapid and stable algorithm to solve the RISM equation, since the typical simulation requires a large number of MC steps, each of which includes recalculation of the solvation free energy. The algorithm developed by Kinoshita et al.[63,64] was implemented to solve the RISM equation, which made the calculation faster by more than a hundred times compared to the standard Picard algorithm. The simulated annealing was employed for the Monte-Carlo sampling. The four conformations depicted in Fig. 6 were taken as the initial guess, which are respectively: (i) the conformation in the global energy minimum in vacuum, which is relatively

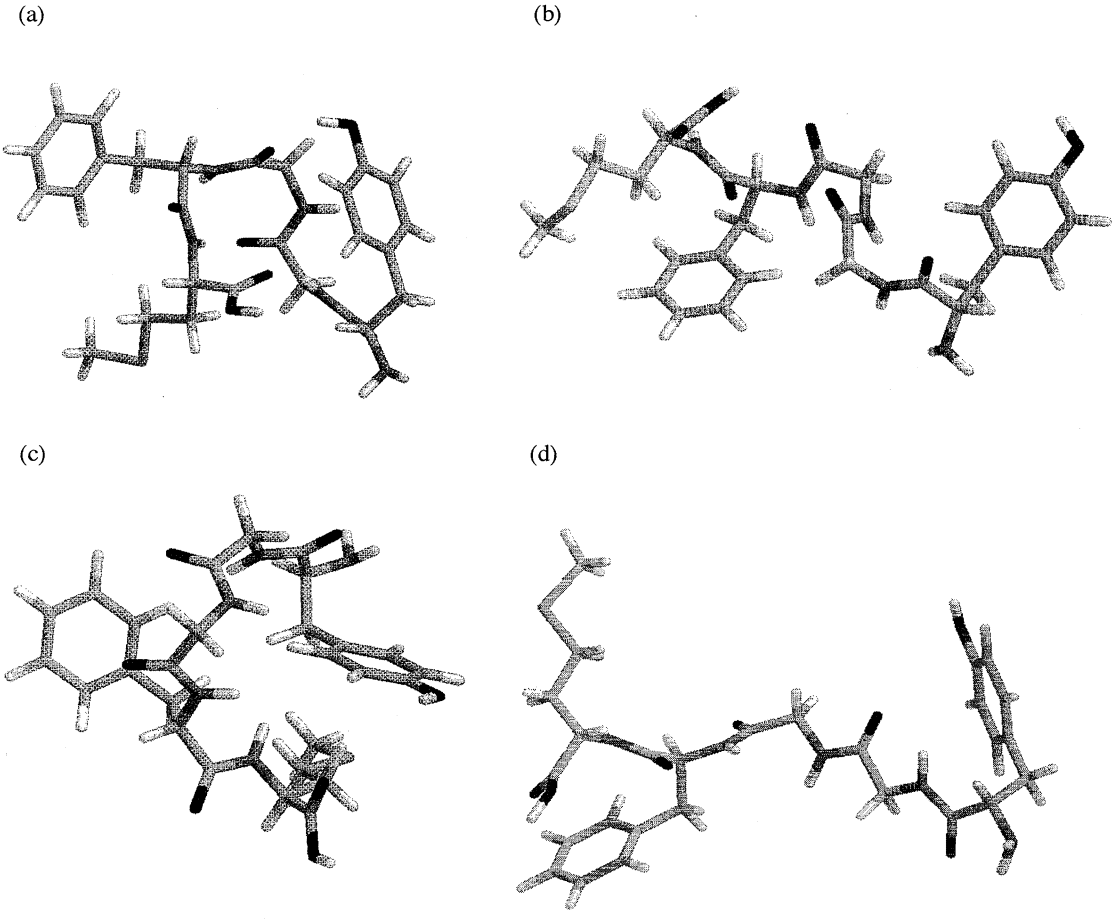

Fig. 6. Initial conformations of Met-enkephalin in the coupled RISM-Monte-Carlo simulation: (a) conformation 1, (b) conformation 2, (c) conformation 3, (d) conformation 4.

compact due to a hydrogen-bond between H^{η} of Tyr^1 side chain and the carbonyl oxygen of Gly^3 backbone;[55,58] (ii) a conformation appeared in a course of other simulation which features large conformational strain and low solvation free energy; (iii) the experimentally observed conformation in the micelle solution, in which oxygen atoms with negative partial charges are located in one side of the molecular plane; (iv) the experimentally observed conformation in water. The last two conformations have been determined from the 2D NMR experiment.[65] $F(\{M\})$, $E_{\mathrm{conf}}(\{M\})$, and $\Delta\mu(\{M\})$ of the four conformations are listed in Table 4. The final conformations obtained from the simulation in the three different environments are exhibited in Fig. 7 as superpositions of the few structures with the lowest energies. The theoretical result obtained in water looks almost identical with the corresponding experimental conformations shown in Fig. 2 in Ref. 65, which is markedly different from neither of the results in the two other environments. Our observation suggests that a proper account of specificity of solvent is crucial in examining the conformational stability of protein.

Table 4. Solvation Free Energies ($\Delta\mu$), Conformational Energies (E_{conf}) and Total Energies ($F=\Delta\mu+E_{\mathrm{conf}}$) (Unit in kcal mol^{-1})

Conf.	$\Delta\mu$	E_{conf}	F
1	196.8	−12.0	184.8
2	178.0	12.2	190.2
3	202.7	−2.5	200.2
4	176.8	0.8	177.6

The results, however, were not surprising for us, since we knew from the preceding study that the minimum energy conformation in vacuum is unstable in water due to the intramolecular hydrogen bond between H^{η} of Tyr^1 side chain and the carbonyl oxygen of Gly^3 backbone, and that the experimentally observed conformation in water is most stable among the four conformations listed above (Table 4).[61] What surprised us is the number of Monte-Carlo steps to be required for converging to the final conformations. The number of Monte-Carlo steps for the convergence in water was one to two orders less than that in the other environments. It appears as if water discriminately discards structures which are unfavored by itself. Plotted in Fig. 8 are the solvation free energies of the four conformations in water and in the non-polar solvent. The difference in the free energies among the conformations is much greater in water than in the non-polar solvent. Moreover, the behavior is not changed when all the partial charges of peptide atoms are removed, which indicates that the discriminative behavior is due to the change in the reorganization free energy of water induced by the solute conformational change. If the finding has any general signif-

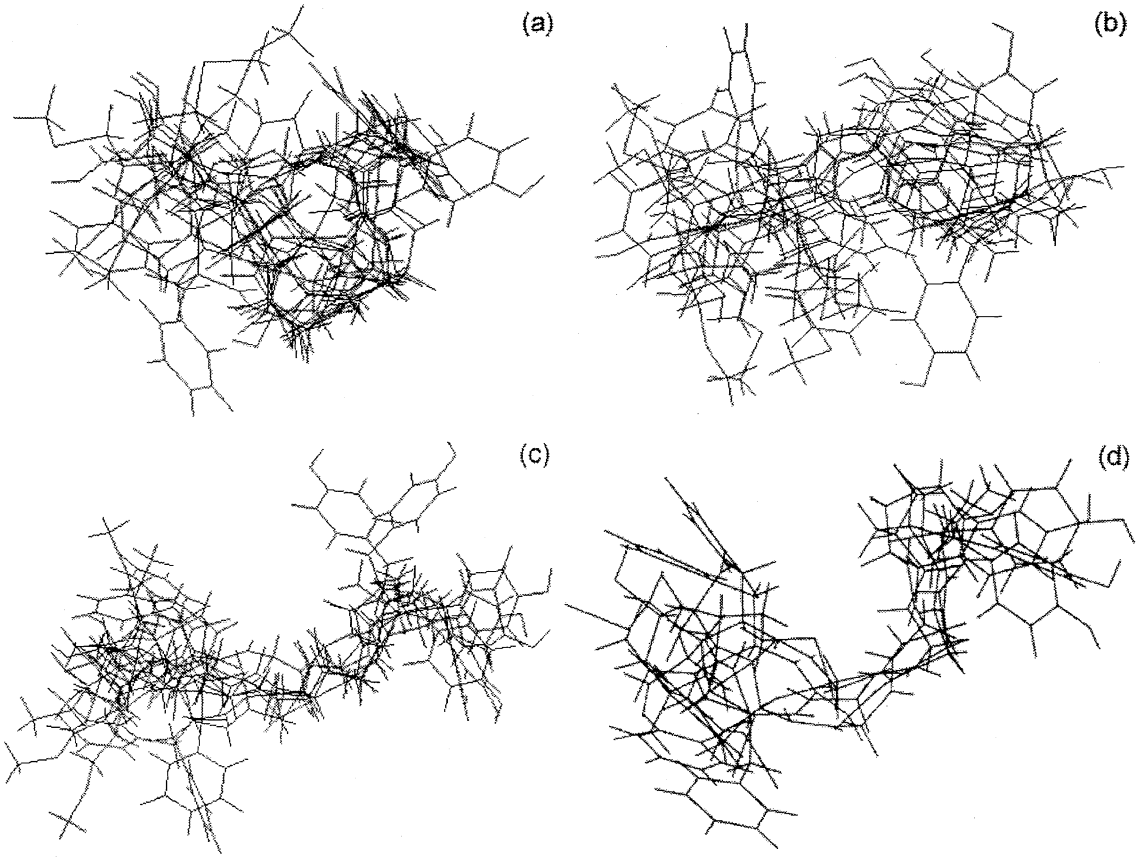

Fig. 7. Superposition of the lowest energy conformations of Met-enkephalin obtained from the simulation in various conditions: (a) in gas phase, (b) in Lennard–Jones fluid, (c) in aqueous solution. The conformations obtained from the NMR experiment are also exhibited for comparison.

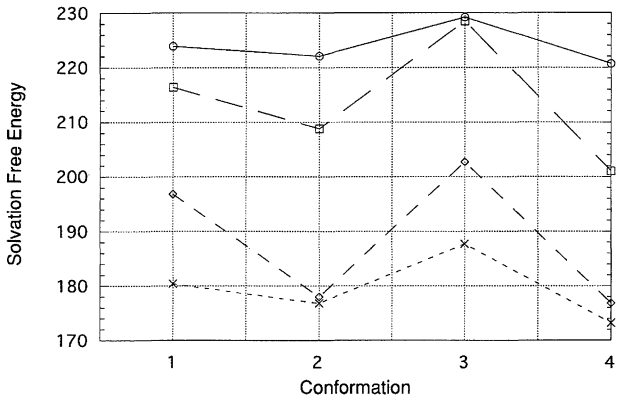

Fig. 8. Solvation free energies of the four conformations (Fig. 6) of Met-enkephalin with and without atomic charges in various environments: ◇, Met-enkephalin with atomic charges in water; □, Met-enkephalin without atomic charges in water; ×, Met-enkephalin in Lennard-Jones fluid; ○, Met-enkephalin in fluid interacting with simple repulsive potential.

icance, we might have touched another important question in protein folding known as the Levinthal paradox, a paradox which has puzzled people in the protein community for a long time.[66] A rough estimation of time required for a protein to fold into its native conformation, based on the number of degrees of freedom in the molecule, is astronomically large, while an actual protein finds its native conformation within a few seconds to a few hours. Although it is highly speculative at the moment, the folding path way of protein may be guided by the discriminative nature of water.

5. Non-equilibrium Solvation Processes in Molecular Liquids

The solvation described so far based on the extended RISM theory involves static or equilibrium properties which are associated with the spatial density fluctuation of solvent molecules around a solute. The latest development in the experimental techniques including the high resolution NMR, and a variety of techniques in the time-resolved laser-spectroscopies, have revealed the molecular nature of the solvent dynamics around solute or the solvation dynamics, which refute any naive interpretation based on the continuum models.[11,12] A microscopic or statistical-mechanical description for the solvation dynamics requires the formulation of temporal as well as spatial fluctuations of solvent density around solute. A general recipe to such a problem is to use the generalized Langenvin equation (GLE).[67] The GLE in principle gives the dynamics of a system in any resolution in space and time depending on the level of projection or coarse graining in the phase space. However, its actual usefulness for a problem is largely determined by a choice of dynamic variables onto which other degrees of freedom are projected. Two fundamental requirements to be considered for the choice of the dynamic variables are tractability and maximum resolution in space and time: The equation should describe the dynamics as detailed as possible in space and time, and yet the equation should be tractable with available theoretical tools. Much attention has been paid in the past to the time resolution, i.e., Markovian or Non-Markovian, in the development of the GLE theory, but not so much to the spatial description. However, the importance of the detailness of the spatial description will probably increase as the dynamics becomes faster, since the mechanical coherence would become important in the short time evolution from an equilibrium state. It is the density–density pair correlation functions which retain the microscopic nature of the system and yet are tractable within the current development in the statistical-mechanical theory of liquids. A natural choice of the dynamic variables which leads to the density–density pair correlation function as an important ingredient in the dynamical equations is a set of the collective density field and its conjugate momentum density field. Such a choice leads to a Smoluchowsky–Vlasov type diffusion equation in the overdamped limit.[68,69]

As to the model for molecular diffusion in polar liquids, there are two quite different points of view. One is the conventional rot-translational model[70—72] and the other the interaction-site description which sees the diffusion of a molecule as a correlated motion of each atom (site).[73,25] The interaction-site description of liquid dynamics can be realized by coupling the RISM equation with the generalized Langevin equation for the site–site density correlation functions. The theories have been successfully applied to calculate the space-time correlation functions of water, and to describe the dynamic Stokes shift in a variety of solvents.[74,75] A remarkable feature of such treatments is an ability to discriminate solvent dynamics according to their chemical specificities reflected in the Hamiltonian. The best example of such discrimination is the two and three step relaxations exhibited in the solvation dynamics of water and methanol, respectively, which were obtained using the same diffusion constant for the solvent.[75]

It is clearly advantageous to use the site–site description compared to the rot-translational model to account for chemical characteristics of solvent as well as solute dynamics. However, the site–site description has its own disadvantage in interpreting physical meaning of the results, since it does not give an explicit picture for the rotational relaxation of molecules, which can be directly probed by many experimental means including the dielectric and NMR relaxations. Chong and Hirata solved the problem by extracting collective modes of the density fluctuation from the site–site density correlation functions.[76]

5.1. Liquid Dynamics Viewed as a Collective Density Fluctuation. Let the density field, $\rho_\alpha(\boldsymbol{r},t) = \sum_i \delta(\boldsymbol{r} - \boldsymbol{r}_i^\alpha(t))$, and the longitudinal current density, $j_\alpha(\boldsymbol{r},t) = \sum_i v_{i,z}^\alpha \delta \times (\boldsymbol{r} - \boldsymbol{r}_i^\alpha(t))$, be the dynamic variables, which are related to each other by the continuity equation,

$$\dot{\rho}_\alpha(\boldsymbol{r},t) = -\nabla j_\alpha(\boldsymbol{r},t). \tag{24}$$

The site–site density correlation function in the Fourier k-space at time t is defined by

$$F_{\alpha\beta}(\boldsymbol{k},t) = \langle \delta\rho_\alpha(\boldsymbol{k},t)\delta\rho_\beta(\boldsymbol{k},0)\rangle, \tag{25}$$

where $\delta\rho_\alpha(\boldsymbol{k},t)=\sum_i e^{i\boldsymbol{k}\cdot\boldsymbol{r}_i^\alpha(t)}$ is the spatial Fourier transform of the density fluctuation of atom α,

$$\delta\rho_\alpha(\boldsymbol{r},t) = \rho_\alpha(\boldsymbol{r},t) - \rho_\alpha. \tag{26}$$

The generalized Langevin equation for $F(k,t)$ is written as

$$\ddot{F}(k,t) + \langle\omega_k^2\rangle F(k,t) + \int_0^t d\tau K_L(k,t-\tau)\dot{F}(k,\tau) = 0, \tag{27}$$

where $\langle\omega_k^2\rangle$ denotes the normalized nth frequency moment matrix of $S(k,\omega)$ defined by the relations,

$$S(k,\omega) = \int_{-\infty}^{\infty} dt e^{i\omega t} F(k,t) \tag{28}$$

$$\overline{\omega_k^n} = \frac{1}{2\pi}\int_{-\infty}^{\infty} d\omega\omega^n S(k,\omega), \tag{29}$$

$$\langle\omega_k^2\rangle = \overline{\omega_k^n} S(k,0)^{-1}. \tag{30}$$

If the damping term is absent, the equation is formally identical to that of the harmonic oscillators, $\ddot{q}+\omega^2 q = 0$. The eigenmodes of the collective density fluctuation, which can be obtained by diagonalizing the matrix $\langle\omega_k^2\rangle$, are identified as acoustic and optical modes of the fluctuation. The eigenfrequencies obtained by diagonalizing $\langle\omega_k^2\rangle$ for a system of diatomic molecules is plotted against the wave vector k in Fig. 9(a). The diatomic molecule A–B is characterized by masses, $m_A = 36$ g mol^{-1}, $m_B = 4$ g mol^{-1}; bond length, $l_{AB} = 2.0$ Å; partial charges, $q_A = -0.25e$, $q_B = +0.25e$; dipole moment, 2.4 D; and L–J parameters: σ_A=4.0 Å, $\sigma_B = 2.0$, ϵ_{AB}=200 K, ϵ_{BB}=100 K. The dispersion relation corresponding to the accoustic mode shows the behavior typical of the monatomic liquid, while that of the other mode does not vanish in the $k\to 0$; to this fact the term "optical" is attributed. The eigenvectors which diagonalize the matrix $\langle\omega_k^2\rangle$ are a linear combination of the atomic density fluctuation $x_A(k)\delta\rho_A(\boldsymbol{k})+x_B(k)\delta\rho_B(\boldsymbol{k})$, where $x_A(k)$ and $x_B(k)$ denote the contribution of each atom to the modes, which depends on the atomic masses and the bond length of a molecule. Plotted in Fig. 9 (b) and (c) are the contributions of each atom to the acoustic and optical modes, respectively. The acoustic mode is dominated by the heavier atom (A) except for the region of long wavelength, where both atoms contribute equally for obvious reasons. On the other hand, the optical mode is governed by the lighter atom (B) over the entire wavelength range, because rotational motion of a molecule is dominated by the motion of the lighter atom which is located further distant from the center of mass, and because the motion is limited in a small region. In the $k\to 0$ limit, the eigen frequencies of those modes for a system of diatomic molecules become in the non-damping limit,

$$\omega_{acou}^2(k\to 0) = \frac{k_B T}{M\chi(k=0)}k^2, \tag{31}$$

and

$$\omega_{opti}^2(k\to 0) = \frac{4k_B T}{3I\chi''(k=0)l_{AB}^2}, \tag{32}$$

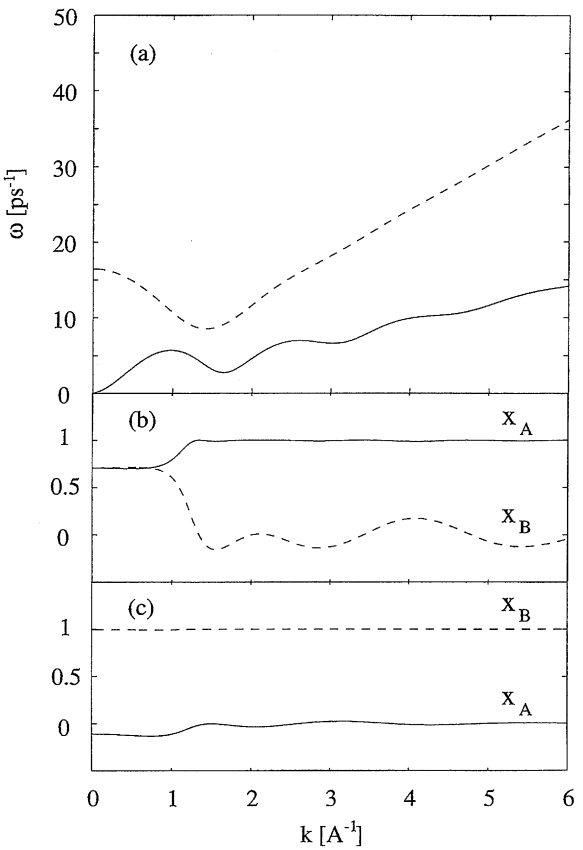

Fig. 9. Eigenfrequencies as evaluated by diagonalizing $\langle\omega_k^2\rangle$. Solid and dashed lines give the eigenfrequencies of the acoustic and optical modes, respectively. (b) x_A (solid line) and x_B (dashed line) defined in the text corresponding to the acoustic mode. (c) x_A (solid line) and x_B (dashed line) defined in the text corresponding to the optical mode. x_A and x_B are normalized such that $x_A^2+x_B^2 = 1$.

respectively, where M, I, and l_{AB} are the total mass, the moment of inertia, and the bond length of the molecule, respectively. $\chi(k=0)$ and $\chi''(k=0)$ denote the zero-th and second moment of the density–density correlation function, $\chi(\boldsymbol{r},\boldsymbol{r})=\langle\delta\rho_\alpha(\boldsymbol{r},t)\delta\rho_\beta(\boldsymbol{r}',0)\rangle$. The $\omega_{acou}^2(k\to 0)$ coinsides with that of the ordinary sound modes propagating with the sound velocity $(K_B T/M\chi(k=0))^{1/2}$ and wave vector $\boldsymbol{k}$.[77] (Remember $\chi(k=0)$ is related to the compressibility, and the sound velocity has a simple relation with the compressibility.) The fact that the expressions include the total mass of a molecule suggests the mode is related to the translational motion of molecules. On the other hand, $\omega_{opti}^2(k\to 0)$ contains the moment of inertia and the bond length, indicating that the quantity is associated with the rotational motions of molecules. The quantity is also related to the dielectric property of liquids, since $\chi''(0)$ is associated with the dielectric constant.[78,79]

As will be demonstrated later, it is more appropriate to use a slightly different basis set from that described above; these are $\delta\rho_N(r,t) = \delta\rho_A(r,t)+\delta\rho_B(r,t)$ and $\delta\rho_Z(r,t) = \delta\rho_A(r,t)-\delta\rho_B(r,t)$. The basis set represents essentially the total number density and the charge density fluctuations, respectively. The number density correlation function in the Fourier k-

space, $F_{NN}(k,t) = \langle \delta\rho_N(k,0) * \delta\rho_N(k,t) \rangle$, which is calculated by assuming a simple exponential decay for the friction kernel, and the charge density correlation functions defined by $F_{ZZ}(k,t) = \langle \delta\rho_Z(k,0) * \delta\rho_Z(k,t) \rangle$ are shown in Fig. 10 for small k. The time constant matrix of the exponential decay was determined by requiring that the resultant $S(k, \omega = 0)$ coincides with $S^G(k, \omega = 0)$ in the $k \to \infty$ limit, where $S^G(k,\omega)$ is the Fourier time-transform of the density–density correlation function in the Gaussian Approximation. The corresponding longitudinal current spectra, defined as

$$C_{L,NN}(k,\omega) = \frac{\omega^2}{k^2} \int_{-\infty}^{\infty} e^{i\omega t} F_{NN}(k,t), \tag{33}$$

$$C_{L,ZZ}(k,\omega) = \frac{\omega^2}{k^2} \int_{-\infty}^{\infty} e^{i\omega t} F_{ZZ}(k,t), \tag{34}$$

which give the spectra of the collective excitation in liquids, are plotted in Fig. 11. $C_{L,NN}(k,\omega)$ for small $k(k = 0.1)$ is dominated by the peak located around $\omega \sim 2ps^{-1}$, which can be identified as the acoustic mode giving a slow and monotonic decay in $F_{NN}(k,t)$. On the other hand, $C_{L,NN}(k,\omega)$ has a single peak around $\omega \sim 21ps^{-1}$, which can be assigned as the optical mode giving a fast and oscillatory behavior in $C_{L,ZZ}(k,\omega)$.

As we have seen, a clear physical picture can be attached to the site–site description of liquid dynamics through the eigenmode analysis of the collective density fluctuations. Nonequilibirum solvation can be described from the same physical viewpoint, which is of special interest in the chemistry in solution. In what follows, an application to the classical problem of ion mobility in polar solvent is explained.

5.2. Dynamics of Solvated Ion in Polar Liquids. An ion in polar liquids is under continuous Brownian motion, and the frictional force exerted on the Brownian particle is

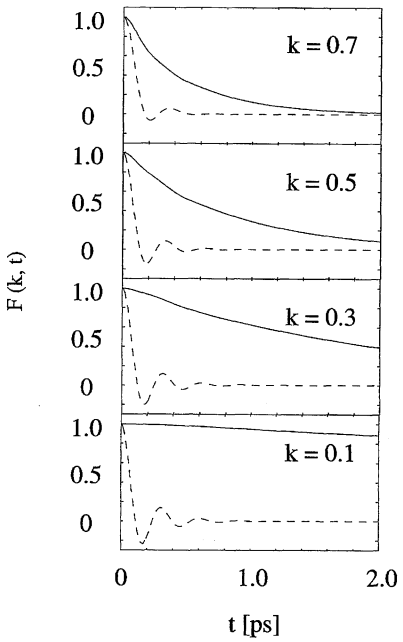

Fig. 10. Normalized $F_{NN}(k,t)$ (solid lines) and $F_{ZZ}(k,t)$ (dashed lines) at the indicated k (in Å^{-1}) values.

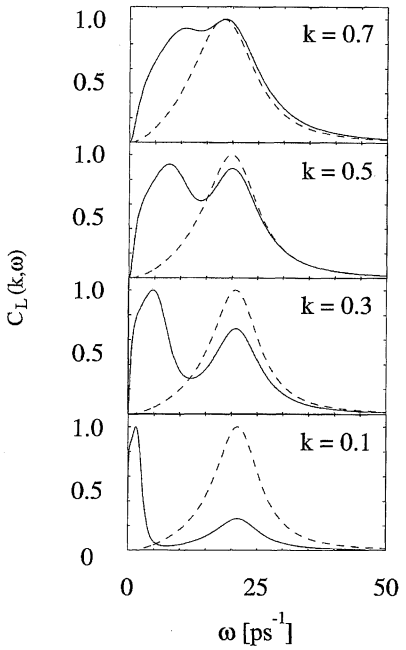

Fig. 11. Longitudinal current spectra, $C_{L,NN}(k,\omega)$ (solid lines) and $C_{L,ZZ}(k,\omega)$ (dashed lines) at the indicated k (in Å^{-1}) values.

proportional to its velocity. The proportional constant, or the friction coefficient, has been a focus of intensive research for almost a hundred years in both experimental and theoretical studies.[80—82,89] According to the simple Stokes law, based on the hydrodynamic theory, the friction should increase proportionally with ionic radii.[5] However, the experimental observations for small ions such as alkai-halide ions in water show a dependency on ion size, which is just opposite to Stokes' law. Concerning origins of the peculiar behavior, two models have been proposed and have coexisted for a long time; these attribute quite different physics to the solvent response to the solute perturbation. The first model maintains the classical view of the Stokes law, but with an "effective" ionic radius, or the Stokes radius, originating from "solvation". In that model, solvent molecules are regarded as firmly bound by the ion, and radius of the solvated ion plays a role of the Stokes radius. The Stokes radius decreases with increasing ionic radius, since the ion-solvent interaction is weakened due to the increased distance. The solvated-ion model has been successful to explain many physico-chemical processes in solutions. The other model for the ionic friction concerns the dielectric response of solvent to the solute perturbation. When an ion is fixed in a polar solvent, the solvent is polarized due to the electrostatic field of the ion. If the ion is displaced, the solvent polarization is not in equilibrium with the new position of the ion, and the relaxation of the polarization should take place in the solvent. The energy dissipation associated with the relaxation process may be identified as friction. The friction decreases with increasing ionic radius, and so, with decreasing electrostatic field of ions. The model developed by Born, Boyd, and Zwanzig has taken a complete theoretical form due to the work by

Hubbard and Onsager by solving an electro-hydrodynamic equation in which the electrostatic as well as hydrodynamic strains are incorporated.[83—86] As far as qualitative aspects of the ion-size dependence of the friction are concerned, which has a minimum with increasing ionic radius, both models stated above explain the experimental observations equally well. Then, one may ask "which model is more faithful to the real physics of the ion friction?" and/or "how do the two effects interplay if both are co-existing?" For instance, use of the same parameter for the effective ion-radius will not be justified since increase in the effective radius should give rise to increase in the Stokes friction but decrease in the dielectric friction. The question should be answered by microscopic theory of solvent fluctuations, not by treatment based on the continuum models.

Here, we address the problem from the response of collective density fluctuations in solvent, described above, to the ionic field.[87] Since the Stokes and dielectric frictions originate basically from the energy dissipation due to the translational and rotational motions, respectively, of solvent, it is reasonable to ask how the ionic field couples with the collective density fluctuations, and/or how the two drag forces are related to the two collective modes. Since the rotational and translational motions of molecules are inherently coupled with each other in our atom-based description of solvent dynamics, the theory is free from artifacts associated with the decoupling of those motions, which is inevitable in the earlier theories based on the explicit orientational coordinates.

Exploiting the standard fluctuation dissipation relations developed by Einstein–Green–Kubo with a mode coupling approximation for a memory kernel in the GLE equation, the friction on an ion exerted from solvent molecules can be expressed as

$$\zeta = \frac{\rho k_B T}{6\pi^2} \sum_{\lambda,\mu} \int_0^\infty dt \int_0^\infty dk k^4 c_{u\lambda}(k) c_{u\mu}(k) F_u(k,t) F_{\lambda\mu}(k,t), \quad (35)$$

where $F_{\lambda\mu}(k,t)$ is the site–site (intermediate) dynamic structure factor of solvent defined in Eq. 25, and $F_u(k,t)$ is the solute dynamic structure factor for which we invoke the diffusion approximation defined by

$$F_u(k,t) = \exp[-Dk^2 t], \quad (36)$$

with the fluctuation dissipation relation,

$$D = k_B T/\zeta. \quad (37)$$

The friction constant ζ can be obtained as a self-consistent solution of Eqs. 35, 36, and 37, which is plotted against the Lennard–Jones radii in Fig. 12. The calculated friction constant has a minimum at a certain ionic radius, which is the general behavior expected from either of the two classical models for the ionic friction mentioned above.

The physical origin of the minimum can be examined in terms of the solute-solvent interactions coupled with the collective density fluctuation in solvent. Changing the dynamic variables from the solvent-atom density $\delta\rho_A(k,t)$ and $\delta\rho_B(k,t)$ to its linear combination, $\delta\rho_N(k,t) = \rho_A(k,t) + \rho_B(k,t)$

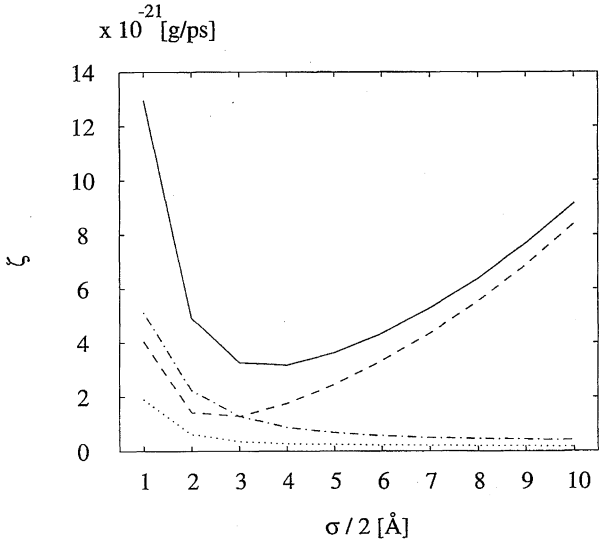

Fig. 12. Decomposition of ζ based on Eq. 38: Solid line, ζ; dashed line, ζ_{NN}; dotted line, ζ_{NZ}; dash-dotted line, ζ_{ZZ}.

and $\rho_Z(k,t) = \rho_A(k,t) - \rho_B(k,t)$, as has been explained above, the friction constant in Eq. 35 is naturally decoupled into three contributions:

$$\zeta = \zeta_{NN} + 2\zeta_{NZ} + \zeta_{ZZ}, \quad (38)$$

where ζ_{NN}, ζ_{ZZ}, and $2\zeta_{NZ}$ respectively represent the short range solute–solvent interaction coupled with the acoustic solvent mode, the long range coulomb interaction with the optical modes, and their cross term. As has been explained above, the acoustic and optical modes represent translational and rotational fluctuation of solvent density; thereby it is natural to associate ζ_{NN} to the Stokes friction and ζ_{ZZ} to the dielectric friction. The three contributions ζ_{NN}, ζ_{ZZ}, and $2\zeta_{NZ}$ are plotted in Fig. 12; they are represented respectively by the dashed, dash-dotted, and dotted lines. The dielectric friction ζ_{ZZ} decreases monotonically with increasing ionic radius. The behavior can be readily interpreted in terms of the electrostic field of the ion, which reduces with increasing ion radius. On the other hand, ζ_{NN} shows rather unexpected behavior in the region of small ionic radius: The friction decreases with increasing ion radius. The unusual behavior can be explained if the short-range interaction between the small ion and solvent molecules is strong enough to make a "solventberg" of which size or life time decreases with increasing the ionic radius. A question may be raised if such a molecular complex can be made only by a short-range interaction. It should be noted that the short-range interaction included in Eq. 35 is not just a bare Lennard–Jones interaction but a renormalized interaction $-kTc_{uv}(r)$ which implicitely includes many body effects due to solvent. Shown in Fig. 13 is the solute-size dependence of the short range part of the direct correlation functions. In the figure, CUi represents an ion with radius i Å. As can be seen, $-kTc_N(r)$ has a quite deep minimum at short ion-solvent separation when the ion size is small (CU1). If the increased Stokes friction for small ion radii is caused by the formation of a solventberg, the

small ions should show different temperature dependence from ions with large radii due to thermal disrupture of the molecular complex. In fact, the ion with the least ionic radius has shown unusually large temperature dependence.[87]

The decoupling in Eq. 38 resembles, in its appearence as well as in its spirit, that made in the seminal work by Wolynes[88] and later made by Bagchi.[89] The new approach, however, should be distinguished from the earlier theories in terms of the level of microscopic description, especially with respect to the structure and dynamics of solvent.

6. Future Prospect

In the present section, the author will try to give some prospective views on the theoretical description of solvation due to the extended RISM theory.

Before doing so, the author wishes to express his opinion on a general question which has often been raised with respect to the importance of the integral equation methods in the liquid state theory. Why does one use the integral equation method to solve the problems when the molecular simulation can replace it in many cases? We can answer the question in two way: one technical and the other more fundamental. Due to the level of complication which characterizes the problems in chemistry, solutions to statistical-mechanical equations are numerical in most of the cases. In that sense, statistical-mechanical equations apparently do not do any better than molecular simulations. However, there are problems in which the molecular simulation fails to give an answer to a question within a reasonable amount of computational resources currently available. A typical example of such questions is the protein folding based on the first principles. For such cases, the difference between the statistical-mechanical theory and the molecular simulations is not just technical but essential. There is an even more fundamental reason to develop the statistical mechanical theories in the chemical processes in solution. Let us explain this point by taking just one example from the solution chemistry. One of the most important findings in the solution chemistry is the so called "square root law" which appears in many of equilibrium and non-equilibrium properties in electrolyte solutions in their concentration dependence: the asymptotic concentration dependence in the lim $C\rightarrow 0$ is proportional to $C^{1/2}$, not to C. As has been clarified by the statistical mechanics of solutions, the limiting behavior is intimately related to the multi-body screening of the Coulomb interaction among charged species. In the typical electrolyte solutions, the Coulomb interaction between a pair of ions asymptotically behaves as $e^{-\varkappa r}/\epsilon r$, that is, the Coulomb interaction is screened by an exponential factor $e^{-\varkappa r}$, where $\varkappa$ is the Debye screening factor, $\varkappa^2=(4\pi\beta/\epsilon)\sum_i q_i^2 c_i$. The square root dependence of the screening constant upon concentrations appearing in the equation is the physical origin of the limiting law. The exponential screening behavior is obtained *mathematically* from the integral equation theory as a renormalization of the coulomb interactions. That is, the physically realized phenomenon of screening has a clear "mathematical" interpretation based on the statistical mechanical theory. Although the molecular simulation may reproduce the exponential behavior of screening in any precision, it will never answer the question why it should be exponential, why it should produce the special concentration dependence for many observable quantities.

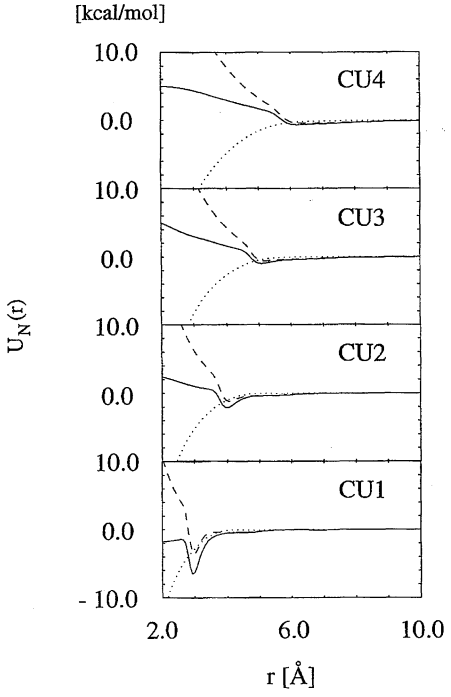

Fig. 13. The effective potential as defined in the text for solutes CU1 to CU4, calculated by the extended RISM equation: Solid lines, $u_N(r)=-k_BTc_N(r)$; dashed lines, contribution from the short range part of $c_{uA}(r)$; dotted lines, contributions from the short range part of $c_{uB}(r)$.

Three important fields in the chemical physics are among the prospects of the extended RISM approach: (1) chemical reaction in solution, (2) biophysical chemistry, (3) solvation dynamics.

There are two aspects in the chemical reaction: the reactivity or chemical equilibrium and the reaction rate. The reactivity of molecules is a synonym of the free energy difference between reactant and product. Most important factors for the reactivity are the changes in the electronic structure and the solvation free energy as long as relatively small molecules are concerned. Those quantities can be evaluated by the coupled quantum and the extended RISM equations; we have seen an example of this in Section 3. The exploration of the reaction dynamics is much more demanding. The reaction dynamics in solutions has two elements to be considered. One of those is the determination of reaction path, the other the time evolution along the reaction path. The reaction path can be determined most naively by calculating the free energy map of reacting species. The RISM-SCF procedure can be employed for such calculations. If the rate-determining step of the reaction is an equilibrium between the reactant and the transition state, the reaction rate can be determined from the free energy difference of the two

states based on the transition state theory. On the other hand, for such a reaction in which dynamics of solvent reorganization determines the reaction rate, the time evolution along the reaction path may be described by a coupled RISM and GLE described in the previous sections with the same spirit as the Kramers theory.[92] Solvent effects on the reactivity and reaction dynamics in organic chemistry are among important applications of such an approach.

Biophysical chemistry is one of the most important fields where the solution chemistry can play a crucial role, since structure and functions of all biomolecules are intimately related to the structure of solvent water. Especially for the tertiary structure of protein, water is essential for determining not only its stability but possibly the rate of folding. In this particular problem, the extended RISM approach is especially superior to the other theories of liquid state, since the approach can take account of the specificity of the molecule in atomic level. In an embryo form, such a calculation has been tried, as shown in Section 3, concerning the conformation of a small peptide in water. Although it requires an enormous amount of computation time, it is encouraging that the equation could be actually solved to give reasonable structural and energetic information for a system with such a large number of interaction sites. It is very likely that the method can be applied to more realistic models of proteins in aqueous solution including electrolytes. The susceptibility of protein stability to the change in thermodynamic variables such as temperature and pressure is among immediate targets for the theory. A key to the successful determination of the tertiary structure of protein in solution will be stable and quick algorithms to solve the equation.

There are many physicochemical processes which are closely related to relaxation processes in liquids, such as the ion transport, the dynamic Stokes shift, and the conformational transition of a molecule in solution. A general concern in modern experimental studies of such phenomena is to analyze the processes in molecular detail or in the level of Hamiltonian. In other words, a theory to describe such phenomena should be able to discriminate chemical specificities of solvent as well as solute on the molecular level. As has been mentioned in the Introduction section, some of recent experimental observations have claimed the necessity of such treatment by demonstrating a breakdown of the continuum model. Nakahara and co-workers have shown that the rotational dynamics of a solute in a variety of solvents does not correlate with the viscosity of the solvent but rather with the solute–solvent interaction.[11] Terazima and his coworkers have found that the diffusion constant of a radical species is roughly a half of that of its parent molecule, which are about the same size.[12] Okada and co-workers observed a clear dicrepancy between the dynamic Stokes shift and the dynamics of the line width.[93] It is very likely that the RISM theory coupled with GLE can give a reasonable account for such phenomena in molecular detail. The slow dynamics in the glass state and the conformational change (isomerization) of a molecule with large degrees of freedom, such as protein, will become targets of the theory in the near future.

The author wishes to express his thank to all his collaborators, especially, to Drs. S. Kato, S. Ten-no, M. Kawata, H. Sato, M. Kinoshita, Y. Okamoto, and Mr. S-H. Chong, who have been deeply engaged in the works presented in the paper. He is also grateful to Drs. K. Arakawa, H. L. Friedman, P. J. Rossky, R. M. Levy, and M. Nakahara, who have given invaluable advice and encouragement to the author for accomplishing his research.

References

1) "Water in Biology, Chemistry and Physics," ed by G. W. Robinson, S. B. Zhu, S. Singh, and M. W. Evans, World Scientific, London (1996).
2) C. Reichardt, in "Solvents and Solvent Effect in Organic Chemistry," VCH, Weinheim (1988).
3) M. Born, *Z. Phys.*, **1**, 45 (1920).
4) L. Onsager, *J. Am. Chem. Soc.*, **58**, 1486 (1936).
5) G. G. Stokes, *Trans. Cambridge Philos. Soc.*, **9**, 8 (1850).
6) A. Einstein, "Investigation on the Theory of the Brownian Movement," ed by R. Fruth, A. D. Cowper, Trans., Dover and New York (1956).
7) P. Debye, "Polar Molecules," Chemical Catalog Company, New York (1929).
8) R. A. Marcus, *J. Chem. Phys.*, **24**, 966 and 979 (1956).
9) J. Tomasi and M. Persico, *Chem. Rev.*, **94**, 2027 (1994).
10) M. K. Gilson and B. Honig, *Nature*, **330**, 84 (1987); J. Warwicker and H. C. Watson, *J. Mol. Biol.*, **157**, 671 (1982); H. Nakamura, *J. Phys. Soc. Jpn.*, **57**, 3702 (1988); W. C. Still, A. Tempczak, R. C. Hawley, and W. Hendrickson, *J. Am. Chem. Soc.*, **112**, 6127 (1990).
11) C. Wakai and M. Nakahara, *J. Chem. Phys.*, **100**, 8347 (1994); **106**, 7512 (1997).
12) M. Terazima and N. Hirota, *J. Chem. Phys.*, **95**, 6490 (1991); M. Terazima, K. Okamoto, and N. Hirota, *J. Phys. Chem.*, **97**, 13387 (1993).
13) M. Maroncelli, *J. Chem. Phys.*, **94**, 2084 (1991).
14) "The Equilibrium Theory of Classical Fluids," ed by H. L. Frisch and J. L. Lebowitz, Benjamin (1964).
15) D. Chandler and H. C. Andersen, *J. Chem. Phys.*, **57**, 1930 (1972).
16) F. Hirata and P. J. Rossky, *Chem. Phys. Lett.*, **83**, 329 (1981); F. Hirata, B. M. Pettitt, and P. J. Rossky, *J. Chem. Phys.*, **77**, 509 (1982); F. Hirata, P. J. Rossky, and B. M. Pettitt, *J. Chem. Phys.*, **78**, 4133 (1983).
17) J. E. Mayer, *J. Chem. Phys.*, **18**, 1426 (1950).
18) A. R. Allnat, *Mol. Phys.*, **8**, 533 (1964).
19) J. C. Rasaiah and H. L. Friedman, *J. Chem. Phys.*, **48**, 2742 (1968).
20) B. M. Pettitt and P. J. Rossky, *J. Chem. Phys.*, **77**, 1452 (1982).
21) F. Hirata, P. Redfern, and R. M. Levy, *Int. J. Quantum Chem: Quantum Bio. Symp.*, **15**, 179 (1988).
22) B. Roux, H. A. Yu, and M. Karplus, *J. Phys. Chem.*, **94**, 4683 (1990).
23) F. Hirata and R. M. Levy, *Chem. Phys. Lett.*, **136**, 267 (1987); *J. Phys. Chem.*, **93**, 479 (1989).
24) R. Chiles and P. J. Rossky, *J. Am. Chem. Soc.*, **106**, 6868 (1984).
25) F. Hirata, *J. Chem. Phys.*, **15**, 4619 (1992).

26) H. L. Friedman, F. Raineri, F. Hirata, and B. Pern, *J. Stat. Phys.*, **78**, 239 (1995).
27) B. M. Pettitt and P. J. Rossky, *J. Chem. Phys.*, **84**, 5836 (1986); J. Perkyns and B. M. Pettitt, *J. Chem. Phys.*, **97**, 7656 (1992).
28) A. Kitao, F. Hirata, and N. Go, *J. Phys. Chem.*, **97**, 10231 (1993).
29) S. J. Singer and D. Chandler, *Mol. Phys.*, **55**, 621 (1985).
30) W. J. Jorgensen and Tirado-Rives, *J. Am. Chem. Soc.*, **110**, 1657 (1988).
31) F. A. Momany, R. F. McGuire, A. W. Burgess, and H. A. Scheraga, *J. Phys. Chem.*, **79**, 2361 (1975); G. Nemethy, M. S. Pottle, and H. A. Scheraga, *J. Phys. Chem.*, **87**, 1883 (1983); M. J. Sipplem, G. Nemethy, and H. A. Scheraga, *J. Phys. Chem.*, **88**, 6231 (1984).
32) W. L. Jorgensen, *J. Am. Chem. Soc.*, **103**, 335 (1981).
33) H. J. C. Berendsen, J. P. M. Postma, W. F. van Gunstern, and J. Hermans, in "Intermolecular Forces," ed by B. Pullman, Reidel, Dortrecht (1981).
34) H. J. C. Berendsen, J. R. Grigera, and T. P. Straatsma, *J. Phys. Chem.*, **91**, 6269 (1987).
35) H. S. Frank, *Discuss. Faraday Soc.*, **24**, 133 (1957).
36) O. Ya. Samilov, *Discuss. Faraday Soc.*, **24**, 141 (1957).
37) K. D. Collins, *Proc. Natl. Acad. Sci. U. S. A.*, **92**, 5553 (1995); K. D. Collins and M. W. Washabaugh, *Q. Rev. Biophys.*, **18**, 323 (1985).
38) Chong and F. Hirata, *J. Phys. Chem.*, **101**, 3209 (1997).
39) H.-A. Yu, B. Roux, and M. Karplus, *J. Chem. Phys.*, **92**, 5020 (1990).
40) C. J. Cramer and D. G. Truhlar, *J. Am. Chem. Soc.*, **113**, 8305 (1991).
41) H. Sato and S. Kato, *J. Mol. Struct. (THEOCHEM)*, **310**, 67 (1994).
42) S. Ten-no, F. Hirata, and S. Kato, *Chem. Phys. Lett.*, **214**, 391 (1993); *J. Chem. Phys.*, **100**, 7443 (1994).
43) H. Sato, F. Hirata, and S. Kato, *J. Chem. Phys.*, **105**, 1546 (1996).
44) M. Kawata, S. Tenno, S. Kato, and F. Hirata, *J. Am. Chem. Soc.*, **117**, 1638 (1995); *Chem. Phys.*, **203**, 53 (1996).
45) M. Kawata, S. Ten-no, S. Kato, and F. Hirata, *J. Phys. Chem.*, **100**, 1111 (1996).
46) S. Maw, H. Sato, S. Ten-no, and F. Hirata, *Chem. Phys. Lett.*, **276**, 20 (1997).
47) H. Sato and F. Hirata, *J. Phys. Chem.*, in press.
48) E. J. King, "Acid Base Equilibria," Pergamon Press, New York (1965).
49) H. Umeyama and K. Morokuma, *J. Am. Chem. Soc.*, **98**, 4400 (1976).
50) M. S. B. Munson, *J. Am. Chem. Soc.*, **87**, 2332 (1965).
51) J. I. Mrauman and L. K. Blair, *J. Am. Chem. Soc.*, **91**, 2126 (1969); J. I. Mrauman, J. M. Riveros, and L. K. Blair, *J. Am. Chem. Soc.*, **93**, 3914 (1971).
52) For example, see articles in "Protein Dynamics," a special issue of Chemical Physics, Vol. 158, (1991).
53) "Mechanism of Protein Folding," ed by R. H. Pain, Springer, New York (1994).
54) B. Anfinsen, E. Haber, M. Sela, and F. H. White, Jr., *Proc. Natl. Acad. Sci. U. S. A.*, **47**, 1309 (1961); C. B. Anfinsen, *Science*, **181**, 223 (1973).
55) M. Vasquez, G. Nemethy, and H. Scheraga, *Chem. Rev.*, **94**, 2183 (1994).
56) S. R. Wilson and W. Cui, "The Protein Folding Problem and Tertiary Structure Prediction," ed by K. M. Mertz, Jr., and S. M. Le Grand, Birkhauser, Boston (1994), pp. 43—70.
57) H. Kawai, T. Kikuchi, and Y. Okamoto, *Protein Eng.*, **3**, 85 (1989).
58) U. H. E. Hansmann and Y. Okamoto, *J. Comput. Chem.*, **14**, 1333 (1993); **A212**, 415 (1994).
59) "Water: A Comprehensive Treatise," ed by F. Franks.
60) D. Bryngelson, J. N. Onuchic, N. D. Socci, and P. G. Wolynes, *Proteins: Struct. Funct. Genet.*, **21**, 167 (1995).
61) M. Kinoshita, Y. Okamoto, and F. Hirata, *J. Chem. Phys.*, **107**, 1586 (1997).
62) M. Kinoshita, Y. Okamoto, and F. Hirata, *J. Am. Chem. Soc.*, in press.
63) M. Kinoshita, Y. Okamoto, and F. Hirata, *J. Comput. Chem.*, **18**, 1320 (1997).
64) M. Kinoshita and F. Hirata, *J. Chem. Phys.*, **104**, 8807 (1997).
65) W. H. Graham, E. S. Carter, II, and R. P. Hickes, *Biopolymers*, **32**, 1755 (1992).
66) C. Levinthal, *J. Chim. Phys.*, **65**, 44 (1965).
67) J. P. Hansen and I. R. McDonald, "Theory of Simple Liquids," Academic, New York (1986).
68) R. Zwanzig, in "Lectures in Theoretical Physics," ed by W. E. Britton, B. W. Downs, and J. Downs, Wiley-Interscience, New York (1961), Vol. III.
69) T. Munakata, *Prog. Theor. Phys.*, **54**, 1635 (1975); *J. Phys. Soc. Jpn.*, **43**, 1762 (1977).
70) D. F. Calef and P. G. Wolynes, *J. Chem. Phys.*, **78**, 4145 (1983).
71) A. Chandra and B. Bagchi, *Chem. Phys. Lett.*, **151**, 47 (1988); *J. Chem. Phys.*, **90**, 1832 and 7338 (1989).
72) D. Wei and G. N. Patey, *J. Chem. Phys.*, **91**, 7113 (1989); **93**, 1399 (1990).
73) F. O. Raineri, Y. Zhou, H. L. Friedman, and G. Stell, *Chem. Phys.*, **152**, 201 (1991).
74) F. O. Raineri, H. Resat, B-C. Perng, F. Hirata, and H. L. Friedman, *J. Chem. Phys.*, **100**, 1477 (1994).
75) F. Hirata, T. Munakata, F. Raineri, and H. L. Friedman, *J. Mol. Liq.*, **65/66**, 15 (1995).
76) S. Chong and F. Hirata, *Phys. Rev. E*, **57**, 1691 (1998).
77) P. G. De Gennes, *Physica*, **25**, 825 (1959).
78) S. Hoye and G. Stell, *J. Chem. Phys.*, **65**, 18 (1976).
79) D. Chandler, *J. Chem. Phys.*, **67**, 1113 (1977).
80) P. G. Wolynes, *Ann. Rev. Phys. Chem.*, **31**, 345 (1980).
81) J. H. Chen and S. A. Adelman, *J. Chem. Phys.*, **72**, 2819 (1980).
82) S. H. Lee and J. G. Rasaiah, *J. Chem. Phys.*, **101**, 6964 (1994).
83) M. Born, *Z. Phys.*, **1**, 221 (1920).
84) R. H. Boyd, *J. Chem. Phys.*, **35**, 1281 (1961).
85) R. Zwanzig, *J. Chem. Phys.*, **35**, 1281 (1961); **52**, 3625 (1970).
86) J. B. Hubbard and L. Onsager, *J. Chem. Phys.*, **67**, 4850 (1977); J. B. Hubbard, *J. Chem. Phys.*, **68**, 1649 (1978).
87) S. H. Chong and F. Hirata, *J. Chem. Phys.*, in press.
88) P. G. Wolynes, *J. Chem. Phys.*, **68**, 473 (1978); P. Colonomos and P. G. Wolynes, *J. Chem. Phys.*, **71**, 2644 (1979).
89) R. Biswas, S. Roy, and B. Bagchi, *Phys. Rev. Lett.*, **75**, 1098 (1995).
90) R. A. Robinson and R. H. Stokes, "Electrolyte Solutions," Reinhold, New York (1958).
91) H. S. Harned and B. B. Owen, "The Physical Chemistry of

Electrolyte Solutions," Butterworth, London (1965).
92) H. A. Kramers, *Physica*, **7**, 284 (1940).
93) K. Nishiyama and T. Okada, *J. Phys. Chem.*, **A101**, 5729 (1997).

Fumio Hirata
Born: March 17, 1947

1971—1974 Graduate school of Hokkaido University
1977 Doctor of Science (Hokkaido University, Chemistry)
1978—1979 Post doctoral fellow (State University New York at Stony Brook)
1979—1981 Post doctoral fellow (University of Texas at Austin)
1981—1984 Researcher in NASAC Co.
1981—1988 Lecturer (Rutgers University)
1988—1989 Research assistant professor (Rutgers University)
1989—1996 Associate professor (Kyoto University)
1996—date Professor (Institute for Molecular Science)